Electron and Electromagnetic Field Dynamics in Nanostructures

Department of Theoretical and Computational Molecular Science
Division of Theoretical Molecular Science I

NOBUSADA, Katsuyuki	Associate Professor
YASUIKE, Tomokazu	Assistant Professor
NODA, Masashi	Post-Doctoral Fellow
YAMADA, Mariko	Secretary

We have developed theoretical methods to calculate photo-induced electron dynamics in nanostructured materials such as nanoparticles, quantum-dot arrays, and adsorbate-surface systems. Specifically, we have developed generalized theory of a light-matter interaction beyond a dipole approximation on the basis of the multipolar Hamiltonian with the aim of understanding the near-field excitation of molecules at the 1 nm scale. We have also studied exciton–polariton transmission in quantum dot waveguides. Furthermore, collectivity of plasmonic excitations in small sodium clusters was investigated in depth. Ultrafast relaxation dynamics of a gold cluster and adsorbate dynamics have been elucidated in collaboration with experimental groups.

1. Near-Field-Induced Optical Force on a Molecule[1)]

We have calculated the near-field-induced optical forces acting on a silver particle mimicked by a jellium model and on C_{60}. The real-time and real-space TDDFT approach combined with the nonuniform light-matter interaction formalism, recently developed by the authors, was employed to accurately calculate the inhomogeneous charge polarization induced by the full multipole interaction with the near field. The induced force is reasonably explained in terms of the polarization and screening charges. The local optical force on the silver particle takes both positive and negative values depending on the spatial distribution of these charges, and the net force becomes attractive as a result of a balance between the polarization and screening charges. The optical force on C_{60} is an order of magnitude smaller than that on the silver particle because of the lesser mobility of the electrons. The energy dependence of the optical force of these particles showed several maxima and minima, indicating that the resonance excitation does not necessarily induce the optical force most efficiently. Such a nonmonotonic energy dependence of the optical force will be utilized when manipulating nanoparticles at the nanometer scale by controlling the near-field frequency. To calculate the optical forces induced by a highly nonuniform electric field in real molecules, a sensible balance of the polarization and screening charges must be determined. The present first-principles TDDFT approach, taking account of full light-matter interactions, can be a powerful tool for optical manipulation in nanostructures.

2. Exciton–Polariton Transmission in Quantum Dot Waveguides[2)]

We have investigated the exciton–polariton energy transfer in bent or branched waveguides consisting of quantum dot arrays and designed the waveguide to facilitate the wave transmission. The efficient wave transformation between the longitudinal and transverse modes occurs in a waveguide bent by the angle smaller than 90° because of the interactions between the more than nearest-neighbor sites. The transmission efficiency lowers by the dispersion in velocity of the wave packet and also by the difference in the group velocity between the longitudinal and transverse waves. The difference in the group velocity is due to the fact that the longitudinal interaction is twice as large as the transverse one. However, the transmission efficiency was found to be sufficiently improved by controlling the interdot distance so as to equalize the longitudinal and transverse interactions. In the branched waveguide, the wave transmission generally decreased because the additional branch path induces the division of the transmission wave. We also found that the wave transmission rather efficiently occurred even in the branched waveguide by optimizing the branch angle so that the two branches bifurcate symmetrically. If there is energy difference (E) of the local exciton states between the adjacent sites, in the absence of thermal relaxation the transmission of the exciton–polariton wave through the sites was suppressed, depending on E. However, it has been clearly demonstrated that the existence of thermal relaxation enables to open a new channel of the transmission along which the exciton–polariton wave cannot transmit through the Coulomb interaction owing to the energy difference. We expect to control transmission paths in more complicated integrated waveguide circuits by changing temperature.

3. Collectivity of Plasmonic Excitations in Small Sodium Clusters with Ring and Linear Structures[3)]

We have quantified the plasmonic excitations in small sodium clusters in terms of collectivity index, which allows us to study the nature of collective motions of electrons in ring and linear-chain geometries. We found that sodium nanostructures generally have plasmonic excitations irrespective of their geometries. The transition density distribution clearly shows that the strong peaks are assigned to the dipolar collective motions. The dipolar motions have three directions, and the energies of the corresponding plasmonic excitations are degenerate for a spherical particle. In the present clusters, the plasmonic excitations split into higher- and lower-energy modes owing to their lower symmetries. The lower-energy mode is attributed to the electronic motion along the direction where the electrons can move through a longer distance. In this case, the clusters have large transition moments although the corresponding collectivity indices are small. Therefore, we regard the lower-energy mode as a long-range charge transfer excitation. In contrast, the higher-energy plasmonic excitation is highly collective as a result of equal-strength interactions among energetically degenerate individual electronic states. In the vicinity of the higher-energy plasmonic excitation, we found that nondipolar collective modes exist. They are expected to play an important role in the interaction between nanoparticles in the context of nano-optics.

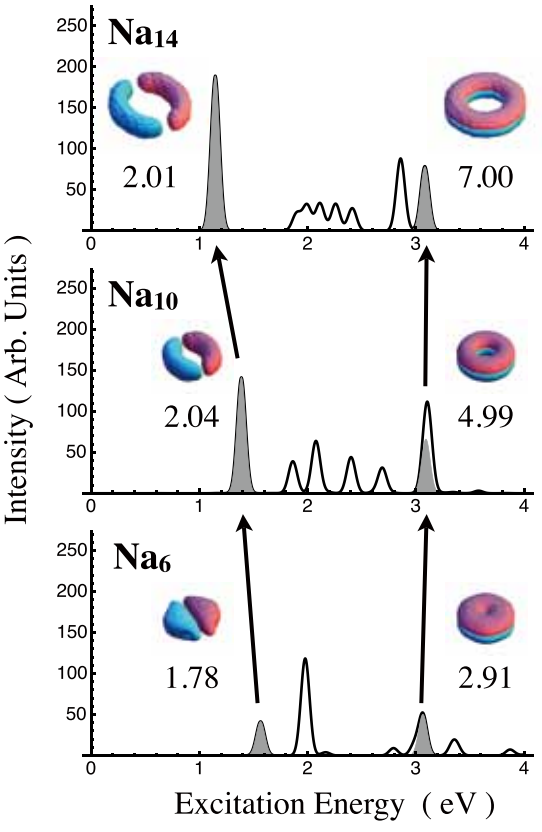

Figure 1. Photoabsorption spectra for ring Na_n clusters (n = 6, 10, and 14). The color insets illustrate the transition density distributions for plasmonic excitations.

4. Ultrafast Relaxation Dynamics of Rod-Shaped 25-Atom Gold Nanoclusters[4)]

We report a femtosecond spectroscopic investigation on the electronic structure and relaxation dynamics of a rod-shaped, 25-atom (Au_{25}) nanocluster capped by organic ligands. Broadband femtosecond transient absorption spectra of the cluster show overlapped excited state absorption and ground state bleach signals. Two lifetimes (*i.e.*, 0.8 ps fast component and a 2.4 μs long component) are identified, with the 0.8 ps component attributed to the fast internal conversion process from LUMO+n to LUMO and the long component to electron relaxation to the ground state. The rod shape of the cluster induces a strong anisotropic response in the transient absorption spectra, from which we deduce that the transition moment is oriented with the long axis of the prolate-shaped cluster. In addition, coherent phonon emission at 26 cm^{-1} was observed and results in the modulation of the excited state absorption transition energy.

5. Adsorbate-Localized versus Substrate-Mediated Excitation Mechanisms for Generation of Coherent Cs–Cu Stretching Vibration at Cu(111)[5)]

Coherent Cs–Cu stretching vibration at a Cu(111) surface covered with a full monolayer of Cs is observed by using time-resolved second harmonic generation spectroscopy, and its generation mechanisms and dynamics are simulated theoretically. While the irradiations with ultrafast pulses at both 400 and 800 nm generate the coherent Cs–Cu stretching vibration at a frequency of 1.8 THz (60 cm^{-1}), they lead to two distinctively different features: The initial phase and the pump fluence dependence of the initial amplitude of coherent oscillation. At 400 nm excitation, the coherent oscillation is nearly cosine-like with respect to the pump pulse and the initial amplitude increases linearly with pump fluence. In contrast, at 800 nm excitation, the coherent oscillation is sine-like and the amplitude is saturated at high fluence. These features are successfully simulated by assuming that the coherent vibration is generated by two different electronic transitions: Substrate d-band excitation at 400 nm and the quasi-resonant excitation between adsorbate-localized bands at 800 nm, *i.e.*, possibly from an alkali-induced quantum well state to an unoccupied state originating in Cs 5d bands or the third image potential state.

References

1) T. Iwasa and K. Nobusada, *Phys. Rev. A* **82**, 043411 (2010).
2) Y. Kubota and K. Nobusada, *J. Chem. Phys.* **134**, 044108 (2011).
3) T. Yasuike, K. Nobusada and M. Hayashi, *Phys. Rev. A* **83**, 013201 (2011).
4) M. Y. Sfeir, H. Qian, K. Nobusada and R. Jin, *J. Phys. Chem. C* **115**, 6200 (2011).
5) K. Watanabe, Y. Matsumoto, T. Yasuike and K. Nobusada, *J. Phys. Chem. A* **115**, 9528 (2011).